Preparation and Characterization of Free-Standing Composite Cellulose-Based Carbon Molecular Sieve Membranes

Tiago Araújo[1,2], Francisco Barbosa[1,2], José M. Sousa[1,2,3], Gabriel Bernardo[1,2] and Adélio Mendes[1,2,*]

[1]*LEPABE - Laboratory for Process Engineering, Environment, Biotechnology and Energy, Faculty of Engineering, University of Porto, Rua Dr. Roberto Frias, 4200-465 Porto, Portugal*

[2]*ALiCE - Associate Laboratory in Chemical Engineering, Faculty of Engineering, University of Porto, Rua Dr. Roberto Frias, 4200-465 Porto, Portugal*

[3]*Chemistry Department, University of Trás-os-Montes e Alto Douro, 1013, 5001-801 Vila Real, Portugal*

Abstract: Carbon membranes with excellent strength and mechanical stability were prepared using a cellulose precursor regenerated from an ionic liquid solution with a low loading of boehmite ceramic nanoparticles, *ca*. 0.1 wt. %. The precursor films show an asymmetrical structure while, after carbonization, the corresponding carbon molecular sieve membranes (c-CMSM) show a dense structure with a uniform thickness of *ca*. 22 μm. The c-CMSM exhibited excellent separation performance, well above the Robeson Upper Bound. The permeability of the c-CMSM to hydrogen increased from 300 to 530 barrer and the H_2/CH_4 permselectivity increased to 473, after adding boehmite nanoparticles. Boehmite nanoparticles act as a microporosity-forming agent without compromising the width of the ultramicropores. The prepared c-CMSM is extremely promising for several applications, namely for hydrogen recovery from methane – H_2/CH_4 (Robeson index: θ =13.5); biogas upgrading – CO_2/CH_4 (θ =6.5); CO_2 removal from combustion flue gas – CO_2/N_2 (θ =1.7); and hydrogen recovery from ammonia processes – H_2/N_2 (θ =4.8).

Keywords: Cellulose, Boehmite nanoparticles, Composite carbon molecular sieve membranes, Gas separation.

1. INTRODUCTION

The separation of molecules is an indispensable process to achieve carbon neutrality [1]. Separation processes currently applied in industry, such as cryogenic distillation and adsorption processes are very energy intensive and have low productivity. Membrane separation processes are an alternative for small and medium-scale industrial applications. Carbon Molecular Sieve Membranes (CMSM) are strong candidates for energy-efficient gas separation due to their superior separation performance and high stability under corrosive and high-temperature (up to *ca.* 200 °C) environments [2]. Potential applications of CMSM include carbon dioxide removal from natural gas/biogas streams, hydrogen recovery from streams with light hydrocarbons, light olefins/paraffins separation, xenon recovery, and air separation, among others [3, 4]. Since the initial work by Koresh and Soffer in the 1980s [5], CMSM has been widely studied [3, 4, 6]. CMSM comprises a rigid pore structure produced by controlled carbonization of a thermosetting polymeric precursor [7]. CMSM presents a bimodal pore size distribution and displays a turbostratic structure with disordered sp^2 hybridized graphitic sheets packed imperfectly [8]. The micropores, formed between the crystalline regions, provide the sorption sites, and the ultramicropores are responsible for the molecular gas sieving, restricting the diffusion of the larger molecules [9]. The exceptional gas separation performance of CMSM is possible due to the combination of this molecular sieving transport with a solution–diffusion mechanism. The CMSM pore size can be tuned for the desired separation application by controlling the carbonization conditions (*e.g.* temperature, atmosphere, soak time or heating rate) and/or modifying the polymer precursor with different pre-treatments [4].

In 2019, our group developed the first CMSM based on an ionic liquid-regenerated cellulose precursor [10]. Tailor-made CMSM with a well-developed microporous structure were prepared from ionic liquid solutions, and these presented separation performances well above the Robeson upper bound. Furthermore, they exhibited better permeability/selectivity balance for several separations than other cellulose-based CMSM. Ionic liquid-regenerated cellulose-based CMSM carbonized at 550 °C presented a permeability to oxygen of 5.2 barrer with an O_2/N_2 permselectivity of 32 and a permeability to H_2 of 206 barrer with an H_2/N_2 permselectivity of 1288 [10]. Very importantly, these CMSM presented the ability to permeate humidified

*Address correspondence to this author at the LEPABE - Laboratory for Process Engineering, Environment, Biotechnology and Energy, Faculty of Engineering, University of Porto, Rua Dr. Roberto Frias, 4200-465 Porto, Portugal; Tel: +351225081695; E-mail: mendes@fe.up.pt

E-ISSN: 2410-1869/22

gas streams due to their high hydrophilicity, a characteristic reported for the first time in this technology [10]. More recently, Araújo *et al*. [11] reported the fabrication of stable cellulose-based CMSM with very high selectivities to H_2/CH_4 and CO_2/CH_4 (> 206,000 and 14,600, respectively) due to the precise tuning of the pore size distribution. The prepared CMSM presented, after 10 days of post-treatment with propylene, stability to oxygen chemisorption even after 1 year of aging at room conditions. By contrast, CMSM without propylene post-treatment displayed a 62 % reduction in the permeability to oxygen after 1 year of exposure to ambient air.

The incorporation of inorganic nanoparticles into the matrix of carbon molecular sieve membranes (composite-CMSM, c-CMSM) was first proposed by Kim *et al*. [12] in 2002 to improve the CMSM separation performance as well as their mechanical, thermal and chemical stability. These authors added metal ions to sulfonated polyimide and observed that the c-CMSM permeabilities increased with the ionic radius of the metal [12, 13]. Other research groups have produced c-CMSM with Ag [14], Pt or Pd nanoparticles [15] or with zeolites [16], silica [17] or with metal cations [18, 19]. All these approaches proved to be efficient and increased the separation performance of the produced carbon membranes.

In 2011, our group produced for the first time c-CMSM with boehmite nanoparticles (γ-AlO(OH)), a low-cost inorganic nanoparticle, used to increase the permeability of the produced carbon membranes [20]. These nanoparticles were incorporated (from a suspension) in a phenolic resin to produce c-CMSM on top of a porous ceramic support. During the carbonization step, the boehmite nanoparticles suffered dehydration and Al_2O_3 nanofillers with 1-2 nm thickness and 10-30 nm long well dispersed on the carbon matrix were formed. Since then, our group has regularly used inorganic boehmite nanoparticles to produce supported c-CMSMs [20-25]. Incorporating boehmite nanoparticles controls the shrinkage of the precursor film during the carbonization process, due to the formation of well-distributed nanowires within the carbon matrix [22]. In 2014, these promising results prompted our group to study the effect of boehmite nanoparticles on carbon membranes [21]. The boehmite concentration in the phenolic resin precursor solution was assessed concerning the pore volume, pore size distribution and separation performance of the prepared membranes. Increasing boehmite concentration increased pore volume and average pore width [21], leading the authors to the conclusion that the concentration of this inorganic filler plays a pivotal role in increasing the porosity of carbon membranes. These structural results were corroborated by the separation performance of the prepared membranes since, due to the increased porosity, the permeability of the carbon membranes to all gases increased with the boehmite concentration. For example, the permeability to C_3H_6 increased from 36 to 776 barrer as the boehmite concentration increased from 0.5 wt. % to 1.2 wt. %, in the precursor dispersion [21]. However, it was also observed a decrease in the corresponding ideal selectivities.

More recently, Poto *et al.* [26], prepared several phenolic resin precursor solutions with different concentrations of boehmite. Due to its hydrophilicity, boehmite was used to increase water adsorption into the porous carbon matrix. The authors found that, during the carbonization step, boehmite partially decomposed into γ-Al_2O_3 nanosheets, increasing the membrane hydrophilicity and consequently improving water vapor permeation up to a boehmite concentration of 1 wt. % [26]. Furthermore, they found that γ-Al_2O_3 nanosheets do not affect the pore size distribution of the membranes in the region of the micropores ($0.6 < d < 2$ nm) but introduce more defects into the carbon matrix, increasing its tortuosity and/or porosity. Gas and water vapor permeability increases up to a boehmite concentration of 0.8 wt. % [26]. Similarly, the selectivity of water vapor to other gases increases with the alumina content. This work demonstrated that the production of c-CMSM with boehmite is promising for removing water vapor from different industrial streams. Rahimalimamaghani *et al.* [27] prepared c-CMSMs with an inorganic filler similar to the boehmite nanoparticles, aluminum acetyl acetonate. The c-CMSM thickness increased as the concentration of the filler in the dipping solution increased. The pore size distribution shifted towards narrower pores with the addition of aluminum acetyl acetonate up to an amount of 4 wt. %. For amounts above 4 wt. %, as with 6 wt. %, larger pores started to appear. Tuning the additive concentration allowed to prepare c-CMSMs with better separation performances due to the presence of more micropores and a narrower micropore size distribution. The c-CMSM selectivity to H_2/N_2 increased *ca.* 5 times with the incorporation of 4 wt. % of aluminum acetyl acetonate [27].

Due to the promising separation results of c-CMSMs, we proposed for the first time the use of

boehmite as an inorganic filler for free-standing carbon molecular sieve membranes prepared from an ionic liquid regenerated cellulose precursor. So far, boehmite nanoparticles have only been used in precursors that are difficult to process and scale and in supported membranes, which are very expensive. In this work, we present inexpensive industrially scalable c-CMSMs with mechanical stability never seen before in this kind of unsupported materials. Some preliminary but promising results in fabricating unsupported c-CMSMs with good to excellent separation performances, namely for hydrogen or carbon dioxide, and good mechanical stability is reported. It demonstrates that inorganic fillers, such as boehmite, besides changing the chemical structure of the carbon membrane surface, can also tune the carbon membrane pore size for the desired separations.

2. EXPERIMENTAL

2.1. Materials

Raw cellulose (wood pulp - degree of polymerization of 450) was provided by Innovia Films Ltd. The ionic liquid, 1-ethyl-3-methylimidazolium acetate (Emimac) (≥ 95 %), was purchased from IoLiTec. Dimethyl sulfoxide (DMSO) (99.9 %) was purchased from Fisher Scientific. The dispersion of boehmite nanoparticles (10 %) with particle size 8-20 nm named *Alumisol* was obtained from Kawaken Fine Chemicals Co. Ltd. Air Liquide supplied hydrogen (99.999 %), carbon dioxide (99.998 %), nitrogen (99.999 %) and methane (99.995 %).

2.2. Membrane Preparation

In this work, c-CMSM precursor films were prepared from an ionic liquid-regenerated cellulose solution loaded with different concentrations of boehmite nanoparticles. A composite polymeric precursor solution was prepared by dissolving cellulose (9.2 wt. %) in a solution of Emimac: DMSO (30:70 wt. %) containing 0.1 wt. % of boehmite nanoparticles by magnetic stirring for ca. 2 h at 90 °C. A standard precursor solution, without boehmite nanoparticles, was also prepared for reference using the same procedure. The polymeric precursor films (with and without boehmite) were prepared in a spin coater (POLOS^{TM}, SPIN150i) with a spin rate of 1200 rpm with an acceleration of 1000 rpm·s^{-1} for 10 seconds. Then the films were coagulated in distilled water at room temperature and washed with distilled water for 1 hour to remove the excess of the ionic liquid [28]. The films were dried overnight at room conditions. Before the carbonization procedure, the dried precursor films were cut in disks with a diameter of 53 mm and placed in a horizontal stainless-steel grid. The precursor films were then carbonized at 550 °C in a quartz tube placed in a horizontal furnace (Termolab TH) with carbon dioxide as a purge gas with a continuous flow rate of 170 mL·min^{-1} following the temperature history used in our previous work [11]. Immediately after the cooling, the prepared CMSMs were glued with epoxy glue (Araldite® rapid) to a circular stainless-steel support.

2.3. Membrane Characterization

2.3.1. Thermogravimetric Analyses (TGA)

TGA of the cellulose precursor films (*ca*. 8 mg), with and without boehmite, were performed using a thermogravimetric balance (NETZSCH STA 449 F3 Jupiter) under 30 mL·min^{-1} continuous nitrogen flow from room temperature until 600 °C, with a heating rate of 10 °C·min^{-1}. The Al_2O_3 loading was confirmed by thermogravimetric analysis under 30 mL·min^{-1} constant air flow from room temperature until 950 °C, with the same heating rate.

2.3.2. Scanning Electron Microscopy (SEM)

A Phenom XL scanning electron microscope was used to acquire surface and cross-section images from the cellulose precursor films and respective CMSMs. Before being analyzed, the samples were coated with Au/Pd using a Leica EM ACE2000 Sputter Coater equipment. Cross-section images were also taken to confirm the CMSM thickness.

2.3.3. X-ray Analysis

The crystal structure of the polymeric films and respective CMSM were studied with X-ray diffraction (XRD) in a Diffractometer Rigaku Smartlab. The data was collected at 2θ angles (7-60°), with a step size of 0.017° using Cu Kα radiation (1.5406 Å). The crystallinity index (I_{Cryst}) of the precursor films was calculated as described by Segal *et al*. [29] with the scattered intensity at the main peak (at 2θ = 20.1°) and the scattered intensity related to the amorphous region (located at 2θ = 14.5°) [30, 31]. The interlayer distance, also known as the *d*-spacing of the CMSMs, was calculated using the Bragg equation [32].

2.3.4. Permeation Experiments

The permeation measurements were performed inside a thermostatic cabinet with temperature control at 25 °C with a feed pressure of *ca*. 1 bar and a permeate pressure of *ca*. 30 mbar. The permeability of

the CMSMs was computed from the time derivative of the permeating pressure assuming ideal gas behavior. The permselectivity of the CMSMs, $\alpha_{i,j}$, was calculated from the permeability ratio of gas species i and j. The Robeson index, θ, was computed to compare the CMSM performance. Detailed information about the permeability measurements and Robeson index can be found in our previous work [11]. The gas permeability was expressed in barrer (1 barrer = 3.39 x 10^{-16} mol·m·m^{-2}·s^{-1}·Pa^{-1}). A digital high-accuracy micrometer from Mitutoyo MDH-25M was used to determine the CMSM and precursor film thickness.

2.3.5. Micropore Characterization

The CMSM and c-CMSM micropore volume (w_0) and characteristic adsorption activation energy (E_0) were obtained by fitting the adsorption equilibrium isotherm of CO_2 at 273 K to the Dubinin-Astakhov (DA) equation [33]. Helium pycnometry was used to measure the CMSMs true density (ρ_S). The dioxide adsorption equilibrium isotherm was obtained using the volumetric method as described elsewhere [34, 35]. Micropore size distribution (MSD) was obtained using the method proposed by Nguyen, and detailed information about this method can be found elsewhere [34, 36, 37].

3. RESULTS AND DISCUSSION

3.1. Preparation of the Composite Carbon Molecular Sieve Membranes

The polymeric precursor shrinks during the carbonization step due to the removal of water and solvents with the release of heteroatoms during the cellulose decomposition. Table **1** indicates the diameter and thickness values of the prepared membranes before and after carbonization.

From Table **1,** the c-CMSM shrank much less than the reference CMSM, 18.9 % vs 35.8 % for the diameter and 42 % vs 50 % for the thickness, respectively. This happens because boehmite nanoparticles reduce the carbon matrix shrinkage during the carbonization process. According to some authors, boehmite nanoparticles suffer dehydration during carbonization and form a well-dispersed Al_2O_3 nanofiller in the carbon matrix, with preferential axial orientation, thus hindering the excessive shrinkage of the membrane [20, 24, 26]. As shown in Figure **1**, free-standing c-CMSM prepared at 550 °C, with a thickness of *ca*. 22 µm, bends without breaking or forming cracks or defects. This remarkable mechanical stability is very unusual for an unsupported flat-sheet CMSM.

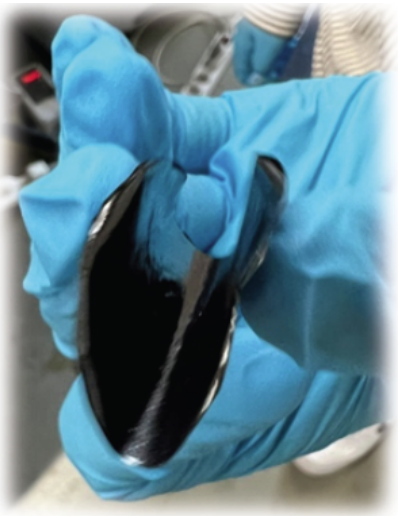

Figure 1: Composite carbon molecular sieve membrane (c-CMSM) after the carbonization at 550 °C.

3.2. Thermogravimetric Analysis

Thermogravimetric analysis was initially used to study the thermal stability and the kinetics of thermal decomposition under an inert atmosphere of the prepared CMSM precursors, after drying. The concerning mass loss curves are plotted in Figure **2**. From this figure, the composite sample loses more mass than the sample without boehmite, up to a temperature of 150 °C. This was assigned to the dehydration of boehmite, already reported by other authors [20, 21]. Table **2** summarizes the main characteristics of the carbonized precursor films. It can

Table 1: Dimensions of the Prepared Cellulosic Precursors, as Placed Inside the Horizontal Furnace (i.e. before Carbonization), and of the Respective Carbon Membranes (i.e. after Carbonization)

	Diameter (mm)		SR (%)	Thickness (µm)		SR (%)
	Precursor	Membrane		Precursor	Membrane	
CMSM	53	34	35.8	36.6	18.3	50
c-CMSM	53	43	18.9	44.2	22.1	42

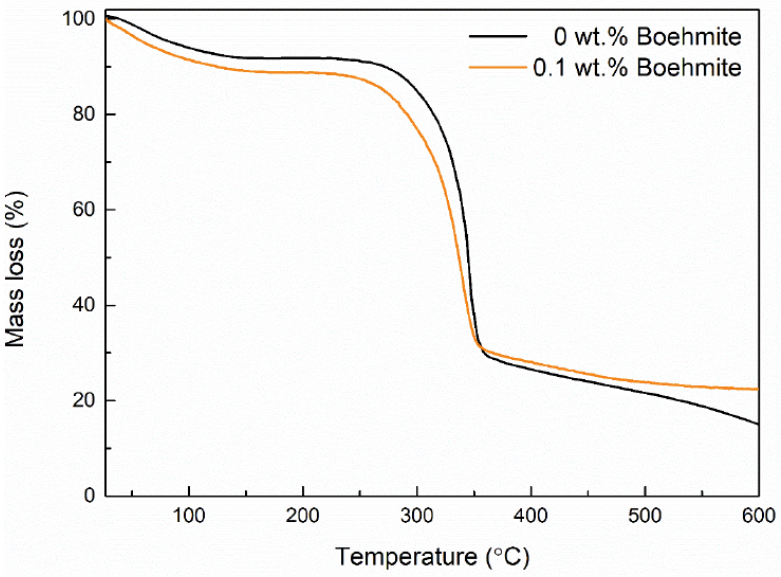

Figure 2: Thermogravimetric analysis of the cellulose and composite precursors.

be observed that the cellulose decomposition temperature of the precursor prepared with boehmite is lower than that of the precursor prepared without boehmite. Regarding the residual mass of the samples at 550 °C, as expected, it is higher for the sample prepared with boehmite nanoparticles, *ca*. 23 % of the initial mass.

Thermogravimetric analysis was also applied to assess the alumina loading in the prepared samples. For this purpose, a TGA of c-CMSM was performed under air flow and the residual alumina fraction at 950 °C was found to be *ca*. 4 wt. %. This alumina fraction value of *ca*. 4 wt. % is expected considering that the initial mass ratio of boehmite to cellulose was *ca*. 1:100. The C/Al_2O_3 fraction obtained was 24.5 %, higher than that reported in the literature for similar materials prepared from phenolic resin and boehmite [21]. This difference was assigned to the fact that CMSMs prepared with phenolic resin have a higher fraction of fixed carbon [20].

Table 2: Summary of the Information Obtained from the TGA of the Produced Samples

	0 % Boehmite	0.1 % Boehmite
Mass loss until 150 °C	8.20	10.9
Residual mass at 550 °C	18.7	22.9
Decomposition temperature (°C)	348	341
γ-Al_2O_3 (%)	-	3.92
C/Al_2O_3	-	24.5

3.3. Scanning Electron Microscopy

The surface and cross-section morphology of the polymeric precursor samples and their carbon membranes carbonized at 550 °C were analyzed by scanning electron microscopy (SEM), *cf*. Figure **3A-D**. Figures **3A** and **3B** show the polymeric precursors. As reported before, the polymeric precursor prepared without boehmite (Figure **3A**) presents a dense structure, while the sample prepared with 0.1 wt. % boehmite (Figure **3B**) shows an asymmetric structure. In Figure **3B** two distinct zones can be seen: an internal zone with high porosity and a very thin dense layer on top. Figure **S1** in supporting information includes an illustrative scheme of this asymmetric structure. A SEM image of the inner porous layer (Figure **S2**) shows a lamellar structure, similar to other asymmetric regenerated cellulose films [38, 39]. Alongside the work performed by Lei *et al*. [40], our work presents the preparation of a polymeric precursor with an asymmetric structure produced from regenerated cellulose. However, a different approach was used in our work, and no post-treatment was applied.

After the carbonization step, both CMSMs present a dense structure (*cf*. Figure **3C-D**); this evidences that the pores shown in Figure **3B** collapse during this step. Modifications in the carbonization step and even pre-treatments will be used in future work to produce c-CMSMs with asymmetric structure. The surface of the samples is smooth, without defects. In the samples prepared with boehmite, there are no visible

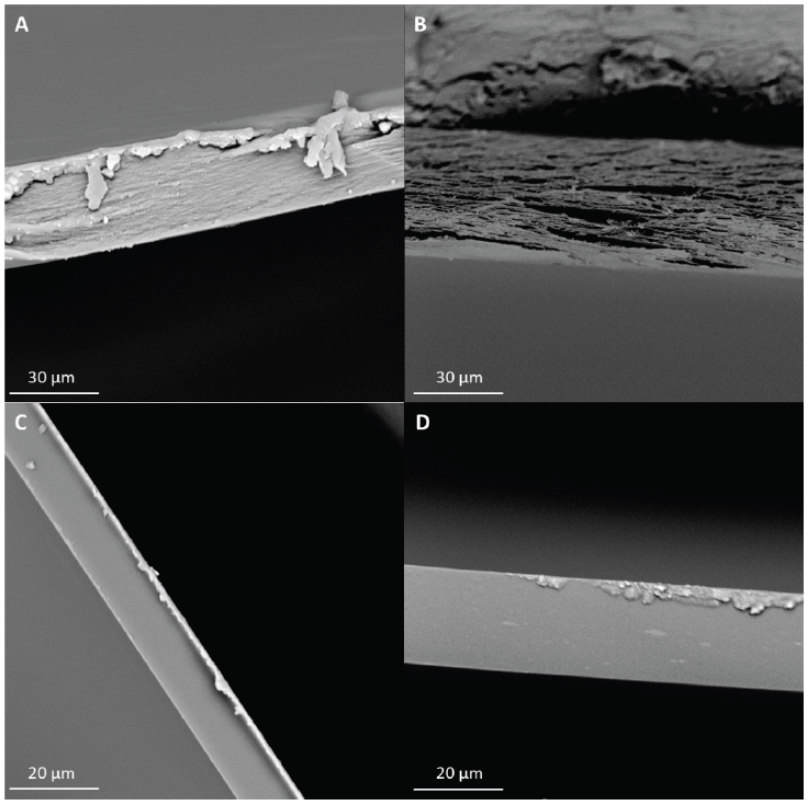

Figure 3: SEM images of the precursor prepared without (**A**) and with 0.1 wt. % of boehmite nanoparticles (**B**); SEM images of the respective CMSM (**C**) and c-CMSM (**D**).

agglomerates of nanoparticles, so it can be concluded that they are well dispersed in the matrix.

3.4. X-ray Diffraction Analysis

The dried precursor films were analyzed using X-ray diffraction (XRD), as shown in Figure **4A**. The main peaks that can be found in these materials are characteristic of cellulose II [41] and are located at 2θ *ca.* 12°, 20° and 21°, which correspond to planes (1 $\bar{1}$ 0), (110) and (020), respectively [41, 42]. As shown in Figure **4A**, adding boehmite to the precursor decreases the intensity of the peaks corresponding to planes (110) and (020) and increases the intensity of the peak corresponding to the plane (1 $\bar{1}$ 0).

The crystallinity index (I_{Cryst}) of the prepared samples was calculated by equation (1) [29]:

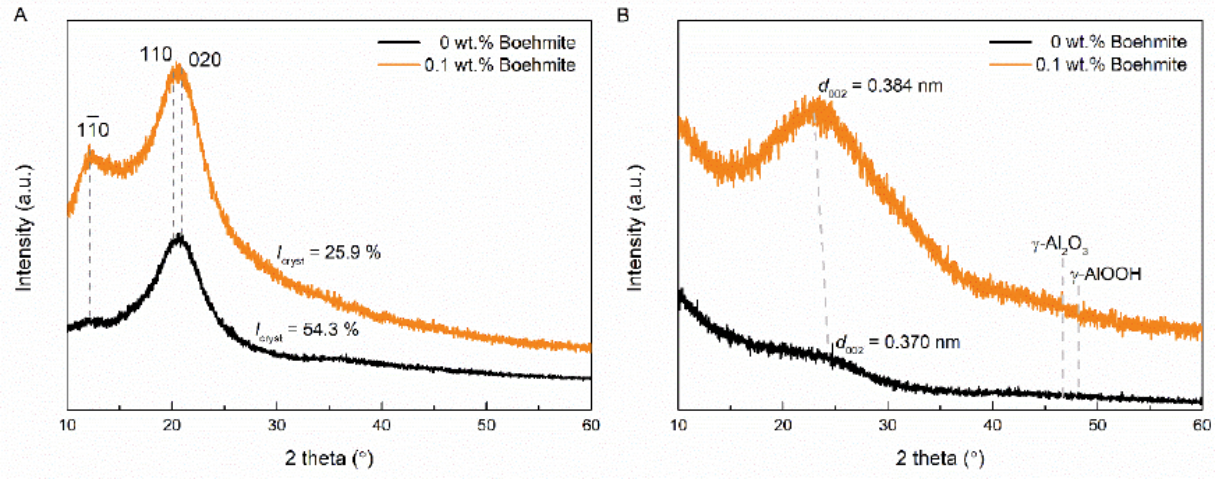

Figure 4: X-ray diffraction of the prepared precursor films (**A**) and the respective XRD patterns for the produced CMSM (**B**).

$$I_{Cryst} = \frac{I_m - I_{am}}{I_m} \quad (1)$$

where I_m is the scattered intensity at the main peak (at 2θ = 20.1°) and I_{am} is the scattered intensity related to the amorphous region (located at 2θ = 14.5° [30, 31]). The I_{Cryst} for the composite precursor is ~ 26 %, about half of the I_{Cryst} of the sample prepared without boehmite nanoparticles (*ca*. 54 %). This result indicates that the nanoparticles reduce the crystallinity of the composite precursor film, increasing the structural disorder of the cellulose polymer chains.

The interlayer distance (*d*-spacing) of the carbonized precursor films was also evaluated by XRD, as illustrated in Figure **4B**. The plane (002) is characteristic of the graphitic domains (sp^2 carbon), at $2\theta \approx 24°$ [32, 40]. The *d*-spacing concerns the distance between neighboring carbon layers [32] and it is not an effective measure of the pore size of the CMSMs; the *d*-spacing was calculated using the Bragg equation:

$$d = \frac{n\lambda}{2\,sin\theta} \quad (2)$$

where d is the d-spacing, n is an integer number, λ is the X-ray wavelength and θ is the diffraction angle [32]. The *d*-spacing increases from 0.370 nm to 0.384 nm on the c-CMSM. The boehmite (γ-AlO(OH)) peak corresponds to the plane (200), which is located at the 2θ value of 48° [43]. Diffraction of γ-Al_2O_3 planes (440) tends to appear at 2θ values of 46° [43]. In Figure **4B**, these peaks are practically imperceptible, which allows us to conclude that the boehmite and γ-Al_2O_3 nanoparticles are well dispersed in the carbon matrix and did not undergo crystallization [26]. This is also because the boehmite concentration is quite small, and the equipment is not sensitive enough to detect these planes. Identical results were reported by Polo *et al*. [26], in which γ-Al_2O_3 and boehmite phases were not detected by XRD in carbon membrane samples with boehmite concentration below 1 wt. %.

3.5. Permeation Results

Different gases were used in the permeation tests of the carbon membranes at 1 bar feed pressure and 25 °C. Figure **5** shows the results of single gas permeation as a function of the correspondent kinetic diameter. Gases with smaller kinetic diameters have greater permeabilities than gases with larger kinetic diameters, therefore the molecular sieve mechanism is preserved by the composite carbon membranes. The permeability of c-CMSM is superior to all gases except to methane. Regarding the c-CMSM permeability to hydrogen, it practically doubled from 305 to 530 barrer with the addition of 0.1 wt. % of boehmite nanoparticles, thus indicating that boehmite can be used to increase the permeability of carbon membranes. With these results, it was concluded that boehmite increases the pore volume since the permeability of c-CMSM increased for all gases except for methane. This feature had already been disclosed by other authors but using supported carbon membranes produced from phenolic resin [21].

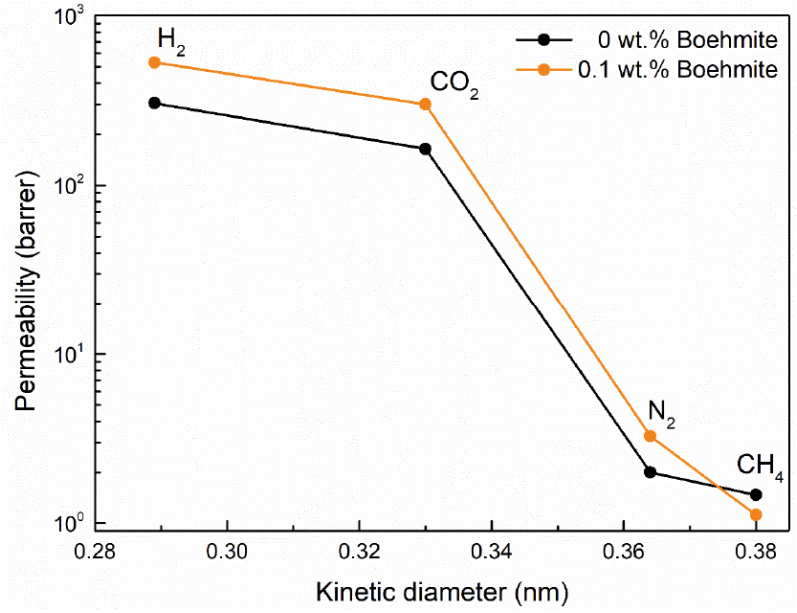

Figure 5: Permeability as a function of the gas kinetic diameter for the prepared CMSM and c-CMSM.

Table 3: Carbon Membrane Permeability, Permsectivity and Respective Robeson Index

	Permeability (barrer)				Permselectivity (-)/Robeson index (-)			
	H_2	CO_2	N_2	CH_4	H_2/N_2	H_2/CH_4	CO_2/N_2	CO_2/CH_4
CMSM	305	164	2.0	1.5	153/3.1	207/3.6	82/1.2	112/2.2
c-CMSM	530	300	3.3	1.1	163/4.8	473/13.5	92/1.7	268/6.5

Table **3** shows the membrane gas permeability, permselectivity and respective Robeson Index for the H_2/N_2, H_2/CH_4, CO_2/N_2 and CO_2/CH_4 separations. Both membranes, with and without boehmite, have a Robeson index value much greater than 1 for these four gas mixtures, meaning that the performance for these separations are well above the Robeson Upper Bound 2008 [44]. Furthermore, and most importantly, composite carbon membranes have selectivities superior to those of carbon membranes without boehmite. It should be noted that the permselectivity for H_2/CH_4 and CO_2/CH_4 more than doubled with the addition of boehmite. Boehmite modifies the structure of the micropores of the membrane, namely increasing its volume, but does not affect the ultramicroporous structure, as will be discussed in the next section, allowing thus a simultaneous increase in the permeability and selectivity of the membranes. The Robeson index for H_2/CH_4 separation has increased from 3.6 to 13.5 with the addition of 0.1 wt. % boehmite (*ca*. 4-fold increase).

This exciting separation performance open the doors to a new investigation pathway; with the addition of a small amount of a low-cost ceramic nanoparticle, the permeability of the membranes increased without harming the selectivities. These c-CMSM are suitable for different separations: recovery of hydrogen from the natural gas network (H_2/CH_4), removal of carbon dioxide from the flue gas (CO_2/N_2) of the combustion process, biogas upgrading (CO_2/CH_4) or hydrogen purification from ammonia processes (H_2/N_2).

3.6. Micropore Characterization

The micropore structure of the prepared carbon membranes was studied by CO_2 adsorption equilibrium isotherm at 0 °C [28]. Figure **6A** presents the CO_2 adsorption isotherm for the carbonized CMSMs. The CO_2 adsorption saturation capacity increases with the boehmite addition to the c-CMSM. The Dubinin-Astakhov's equation (DA equation) was fitted to the experimental data and the micropore volume (w_0) and the characteristic energy of adsorption (E_0) were obtained and are indicated in Table **4**. The mean pore size (ℓ_0) of the prepared carbon membranes was obtained from the average of the micropore size distribution.

Table 4: Micropore Characterization and Structural Parameters were Obtained by Fitting the DA Equation to the CO2 Equilibrium Isotherm

	CMSM	c-CMSM
ρ_S ($g \cdot cm^{-3}$)	2.173	3.576
w_0 ($cm^3 \cdot g^{-1}$)	0.197	0.425
E_0 ($kJ \cdot mol^{-1}$)	32.52	31.02
l_0 (nm)	0.742	0.775

The structural density of the c-CMSM sample – ρ_S – was obtained by He pycnometry and the value obtained was higher for the carbon membrane without boehmite (Table **4**). This increase reflects the large contribution of the boehmite nanoparticles to the mass of the sample (density of boehmite ~3.0). On the other hand, adding only 0.1 wt. % of boehmite nanoparticles the micropore volume increased from 0.197 $cm^3 \cdot g^{-1}$ to 0.425 $cm^3 \cdot g^{-1}$, an increase of 115 %. This micropore volume of the c-CMSM is slightly higher than that obtained for other cellulose based CMSM [11, 40]. The characteristic adsorption energy is lower for the c-CMSM. This indicates that the potential energy of interaction between CO_2 and the c-CMSM walls became lower, with the increase in the micropore volume and their average pore width [31].

The method proposed by Nguyen *et al*. [36, 37] to obtain the micropore size distribution for microporous carbon-based materials was applied – Figure **6B**. As expected, the prepared membranes present a typical bimodal pore size distribution, micropores in the range of 0.7-1 nm and ultramicropores from 0.35-0.7 nm [9, 45, 46]. The c-CMSM presents a higher micropore fraction in the range of the micropores and

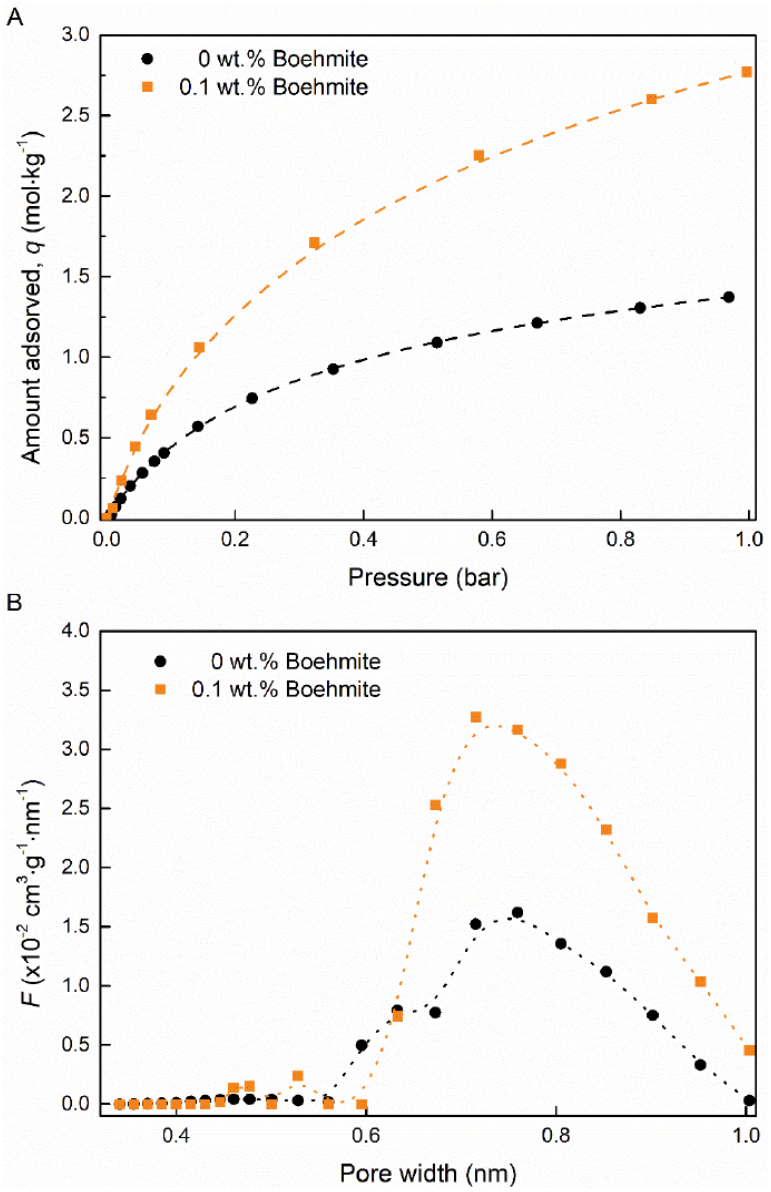

Figure 6: CO_2 adsorption equilibrium isotherms obtained at 0 °C (**A**) and micropore size distribution of the prepared CMSMs (**B**).

ultramicropores and has a more precise cut-off pore size between micropores and ultramicropores which supports the higher gas selectivities. Boehmite nanoparticles play an outstanding role as a pore forming-agent, increasing the micropore volume. The average micropore size (ℓ_0 – Table **4**) increase is insignificant in the carbon membrane prepared with the boehmite nanoparticles. This agrees with the gas permeation results obtained in section 3.4: the permeability of the c-CMSM increased while the selectivity stays approximately constant. Although the micropore volume has more than doubled, the average size of the micropores remained mostly constant.

4. CONCLUSIONS

Unsupported composite cellulose-based carbon molecular sieve membranes were successfully prepared for the first time. The composite carbon membranes were fabricated using a renewable and low-cost polymer precursor of cellulose, loaded with a small amount of ceramic boehmite nanoparticles, in one carbonization step at 550 °C without pre- or post-treatments. The prepared c-CMSMs displayed great separation indications for H_2/CH_4 and CO_2/CH_4 gas separations and exceptional mechanical robustness.

The prepared composite precursor film displayed a lower crystallinity index, as obtained by XRD, and the final c-CMSM presents a lower shrinkage ratio due to the well-dispersed boehmite nanoparticles, which prevent the excessive shrinkage of the membrane. Adding boehmite nanoparticles to prepare cellulosic carbon membranes can be a useful strategy to increase their microporosity. The c-CMSM presents higher separation performance to the different gas molecules when compared with the CMSM prepared without boehmite nanoparticles. The c-CMSM permeability to hydrogen doubled to 530 barrer, the H_2/CH_4 permselectivity increased from 207 to 473, and the CO_2/CH_4 permsectivity increased from 112 to 268. The preparation of this c-CMSM allowed to increase the Robeson index for H_2/CH_4 separation from 3.6 to 13.5.

ACKNOWLEDGEMENTS

T. Araújo is grateful to the Portuguese Foundation for Science and Technology (FCT) for the doctoral grant (SFRH/BD/143598/2019) supported by POPH/FSE. G. Bernardo thanks the Portuguese Foundation for Science and Technology (FCT) for the financial support of his work contract through the Scientific Employment Stimulus Individual Call – (CEEC_IND/02039/2018). This work was financially supported by LA/P/0045/2020 (ALiCE), UIDB/00511/2020 and UIDP/00511/2020 (LEPABE), funded by national funds through FCT/MCTES (PIDDAC). The authors thank Innovia Films Ltd. for generously providing the wood pulp.

REFERENCES

[1] D.S. Sholl, R.P. Lively, Seven chemical separations to change the world, Nature 532 (2016) 435-437. https://doi.org/10.1038/532435a

[2] J.E. Koresh, A. Soffer, The Carbon Molecular Sieve Membranes. General Properties and the Permeability of CH4/H2 Mixture, Separation Science and Technology 22(2-3) (1987) 973-982. https://doi.org/10.1080/01496398708068993

[3] L. Lei, L. Bai, A. Lindbråthen, F. Pan, X. Zhang, X. He, Carbon membranes for CO2 removal: Status and perspectives from materials to processes, Chemical Engineering Journal 401 (2020) 126084. https://doi.org/10.1016/j.cej.2020.126084

[4] T. Araújo, G. Bernardo, A. Mendes, Cellulose-Based Carbon Molecular Sieve Membranes for Gas Separation: A Review, Molecules 25(15) (2020). https://doi.org/10.3390/molecules25153532

[5] J.E. Koresh, A. Sofer, Molecular Sieve Carbon Permselective Membrane. Part I. Presentation of a New Device for Gas Mixture Separation, Separation Science and Technology 18(8) (1983) 723-734. https://doi.org/10.1080/01496398308068576

[6] G. Bernardo, T. Araújo, T. da Silva Lopes, J. Sousa, A. Mendes, Recent advances in membrane technologies for hydrogen purification, International Journal of Hydrogen Energy 45(12) (2020) 7313-7338. https://doi.org/10.1016/j.ijhydene.2019.06.162

[7] M. Rungta, G.B. Wenz, C. Zhang, L. Xu, W. Qiu, J.S. Adams, W.J. Koros, Carbon molecular sieve structure development and membrane performance relationships, Carbon 115 (2017) 237-248. https://doi.org/10.1016/j.carbon.2017.01.015

[8] M. Kiyono, P.J. Williams, W.J. Koros, Generalization of effect of oxygen exposure on formation and performance of carbon molecular sieve membranes, Carbon 48(15) (2010) 4442-4449. https://doi.org/10.1016/j.carbon.2010.08.003

[9] K.M. Steel, W.J. Koros, Investigation of porosity of carbon materials and related effects on gas separation properties, Carbon 41(2) (2003) 253-266. https://doi.org/10.1016/S0008-6223(02)00309-3

[10] S.C. Rodrigues, M. Andrade, J. Moffat, F.D. Magalhaes, A. Mendes, Preparation of carbon molecular sieve membranes from an optimized ionic liquid-regenerated cellulose precursor, Journal of Membrane Science 572 (2019) 390-400. https://doi.org/10.1016/j.memsci.2018.11.027

[11] T. Araújo, M. Andrade, G. Bernardo, A. Mendes, Stable cellulose-based carbon molecular sieve membranes with very high selectivities, Journal of Membrane Science 641 (2022) 119852. https://doi.org/10.1016/j.memsci.2021.119852

[12] Y.K. Kim, H.B. Park, Y.M. Lee, Synthesis and characterization of metal-containing sulfonated polyimide membranes and their gas separation properties, Desalination 145(1) (2002) 389-392. https://doi.org/10.1016/S0011-9164(02)00442-3

[13] Y.K. Kim, H.B. Park, Y.M. Lee, Carbon molecular sieve membranes derived from metal-substituted sulfonated polyimide and their gas separation properties, Journal of Membrane Science 226(1) (2003) 145-158. https://doi.org/10.1016/j.memsci.2003.08.017

[14] J.N. Barsema, J. Balster, V. Jordan, N.F.A. van der Vegt, M. Wessling, Functionalized Carbon Molecular Sieve membranes containing Ag-nanoclusters, Journal of Membrane Science 219(1) (2003) 47-57. https://doi.org/10.1016/S0376-7388(03)00176-5

[15] S. Yoda, A. Hasegawa, H. Suda, Y. Uchimaru, K. Haraya, T. Tsuji, K. Otake, Preparation of a Platinum and Palladium/Polyimide Nanocomposite Film as a Precursor of Metal-Doped Carbon Molecular Sieve Membrane via Supercritical Impregnation, Chemistry of Materials 16(12) (2004) 2363-2368. https://doi.org/10.1021/cm0349250

[16] Q. Liu, T. Wang, H. Guo, C. Liang, S. Liu, Z. Zhang, Y. Cao, D.S. Su, J. Qiu, Controlled synthesis of high performance carbon/zeolite T composite membrane materials for gas separation, Microporous and Mesoporous Materials 120(3) (2009) 460-466. https://doi.org/10.1016/j.micromeso.2008.12.029

[17] H.B. Park, C.H. Jung, Y.K. Kim, S.Y. Nam, S.Y. Lee, Y.M. Lee, Pyrolytic carbon membranes containing silica derived from poly(imide siloxane): the effect of siloxane chain length on gas transport behavior and a study on the separation of mixed gases, Journal of Membrane Science 235(1) (2004) 87-98. https://doi.org/10.1016/j.memsci.2004.01.025

[18] M. Yoshimune, I. Fujiwara, H. Suda, K. Haraya, Gas transport properties of carbon molecular sieve membranes derived from metal containing sulfonated poly(phenylene oxide), Desalination 193(1) (2006) 66-72. https://doi.org/10.1016/j.desal.2005.04.138

[19] J.A. Lie, M.-B. Hägg, Carbon membranes from cellulose and metal loaded cellulose, Carbon 43(12) (2005) 2600-2607. https://doi.org/10.1016/j.carbon.2005.05.018

[20] M. Teixeira, M.C. Campo, D.A. Pacheco Tanaka, M.A. Llosa Tanco, C. Magen, A. Mendes, Composite phenolic resin-based carbon molecular sieve membranes for gas separation, Carbon 49(13) (2011) 4348-4358. https://doi.org/10.1016/j.carbon.2011.06.012

[21] M. Teixeira, S.C. Rodrigues, M. Campo, D.A. Pacheco Tanaka, M.A. Llosa Tanco, L.M. Madeira, J.M. Sousa, A. Mendes, Boehmite-phenolic resin carbon molecular sieve membranes-Permeation and adsorption studies, Chemical Engineering Research and Design 92(11) (2014) 2668-2680. https://doi.org/10.1016/j.cherd.2013.12.028

[22] M. Teixeira, M. Campo, D.A. Tanaka, M.A. Tanco, C. Magen, A. Mendes, Carbon-Al2O3-Ag composite molecular sieve membranes for gas separation, Chemical Engineering Research and Design 90(12) (2012) 2338-2345. https://doi.org/10.1016/j.cherd.2012.05.016

[23] S.C. Rodrigues, R. Whitley, A. Mendes, Preparation and characterization of carbon molecular sieve membranes based on resorcinol-formaldehyde resin, Journal of Membrane Science 459 (2014) 207-216. https://doi.org/10.1016/j.memsci.2014.02.013

[24] M.A. Llosa Tanco, D.A. Pacheco Tanaka, S.C. Rodrigues, M. Texeira, A. Mendes, Composite-alumina-carbon molecular sieve membranes prepared from novolac resin and boehmite. Part I: Preparation, characterization and gas permeation studies, International Journal of Hydrogen Energy 40(16) (2015) 5653-5663. https://doi.org/10.1016/j.ijhydene.2015.02.112

[25] M.A. Llosa Tanco, D.A. Pacheco Tanaka, A. Mendes, Composite-alumina-carbon molecular sieve membranes prepared from novolac resin and boehmite. Part II: Effect of the carbonization temperature on the gas permeation properties, International Journal of Hydrogen Energy 40(8) (2015) 3485-3496. https://doi.org/10.1016/j.ijhydene.2014.11.025

[26] S. Poto, J.G.H. Endepoel, M.A. Llosa-Tanco, D.A. Pacheco-Tanaka, F. Gallucci, M.F. Neira d'Angelo, Vapor/gas separation through carbon molecular sieve membranes: Experimental and theoretical investigation, International Journal of Hydrogen Energy 47(21) (2022) 11385-11401. https://doi.org/10.1016/j.ijhydene.2021.10.155

[27] A. Rahimalimamaghani, D.A. Pacheco Tanaka, M.A. Llosa Tanco, F. Neira D'Angelo, F. Gallucci, Effect of aluminium acetyl acetonate on the hydrogen and nitrogen permeation of carbon molecular sieves membranes, International Journal of Hydrogen Energy 47(32) (2022) 14570-14579. https://doi.org/10.1016/j.ijhydene.2022.02.198

[28] S.C. Rodrigues, M. Andrade, J. Moffat, F.D. Magalhães, A. Mendes, Preparation of carbon molecular sieve membranes from an optimized ionic liquid-regenerated cellulose precursor, Journal of Membrane Science 572 (2019) 390-400. https://doi.org/10.1016/j.memsci.2018.11.027

[29] L. Segal, J.J. Creely, A.E. Martin, C.M. Conrad, An Empirical Method for Estimating the Degree of Crystallinity of Native Cellulose Using the X-Ray Diffractometer, Textile Research Journal 29(10) (1959) 786-794. https://doi.org/10.1177/004051755902901003

[30] Y. Liu, Y. Nie, F. Pan, L. Zhou, X. Ji, Z. Kang, S. Zhang, Study on ionic liquid/cellulose/coagulator phase diagram and its application in green spinning process, Journal of Molecular Liquids 289 (2019) 111127. https://doi.org/10.1016/j.molliq.2019.111127

[31] L. Lei, A. Lindbråthen, X. Zhang, E.P. Favvas, M. Sandru, M. Hillestad, X. He, Preparation of carbon molecular sieve membranes with remarkable CO2/CH4 selectivity for high-pressure natural gas sweetening, Journal of Membrane Science 614 (2020) 118529. https://doi.org/10.1016/j.memsci.2020.118529

[32] Y.K. Kim, H.B. Park, Y.M. Lee, Preparation and characterization of carbon molecular sieve membranes derived from BTDA-ODA polyimide and their gas separation properties, Journal of Membrane Science 255(1) (2005) 265-273. https://doi.org/10.1016/j.memsci.2005.02.002

[33] A. Gil, P. Grange, Application of the Dubinin-Radushkevich and Dubinin-Astakhov equations in the characterization of microporous solids, Colloids and Surfaces A: Physicochemical and Engineering Aspects 113(1) (1996) 39-50. https://doi.org/10.1016/0927-7757(96)81455-5

[34] S.C. Rodrigues, M. Andrade, J. Moffat, F.D. Magalhaes, A. Mendes, Carbon Membranes with Extremely High Separation Factors and Stability, Energy Technology 7(4) (2019). https://doi.org/10.1002/ente.201801089

[35] J.C. Santos, F.D. Magalhães, A. Mendes, Contamination of Zeolites Used in Oxygen Production by PSA: Effects of Water and Carbon Dioxide, Industrial & Engineering Chemistry Research 47(16) (2008) 6197-6203. https://doi.org/10.1021/ie800024c

[36] C. Nguyen, D.D. Do, Adsorption of Supercritical Gases in Porous Media: Determination of Micropore Size Distribution, The Journal of Physical Chemistry B 103(33) (1999) 6900-6908. https://doi.org/10.1021/jp9906536

[37] C. Nguyen, D.D. Do, K. Haraya, K. Wang, The structural characterization of carbon molecular sieve membrane (CMSM) via gas adsorption, Journal of Membrane Science 220(1) (2003) 177-182. https://doi.org/10.1016/S0376-7388(03)00219-9

[38] W.T. Fonseca, R.F. Santos, J.N. Alves, S.D. Ribeiro, R.M. Takeuchi, A.L. Santos, R.M.N. Assunção, G.R. Filho, R.A.A. Muñoz, Square-Wave Voltammetry as Analytical Tool for Real-Time Study of Controlled Naproxen Releasing from Cellulose Derivative Materials, Electroanalysis 27(8) (2015) 1847-1854. https://doi.org/10.1002/elan.201500011

[39] I. Peixoto, M. Faria, M.C. Gonçalves, Synthesis and Characterization of Novel Integral Asymmetric Monophasic Cellulose-Acetate/Silica/Titania and Cellulose-Acetate/Titania Membranes, Membranes, 2020. https://doi.org/10.3390/membranes10090195

[40] L. Lei, F. Pan, A. Lindbråthen, X. Zhang, M. Hillestad, Y. Nie, L. Bai, X. He, M.D. Guiver, Carbon hollow fiber membranes for a molecular sieve with precise-cutoff ultramicropores for superior hydrogen separation, Nature Communications 12(1) (2021) 268. https://doi.org/10.1038/s41467-020-20628-9

[41] J. Gong, J. Li, J. Xu, Z. Xiang, L. Mo, Research on cellulose nanocrystals produced from cellulose sources with various polymorphs, RSC Advances 7(53) (2017) 33486-33493. https://doi.org/10.1039/C7RA06222B

[42] A.D. French, Idealized powder diffraction patterns for cellulose polymorphs, Cellulose 21(2) (2014) 885-896. https://doi.org/10.1007/s10570-013-0030-4

[43] X. Zhang, M. Honkanen, E. Levänen, T. Mäntylä, Transition alumina nanoparticles and nanorods from boehmite nanoflakes, Journal of Crystal Growth 310(15) (2008) 3674-3679. https://doi.org/10.1016/j.jcrysgro.2008.05.016

[44] L.M. Robeson, The upper bound revisited, Journal of Membrane Science 320(1) (2008) 390-400. https://doi.org/10.1016/j.memsci.2008.04.030

[45] V.C. Geiszler, W.J. Koros, Effects of Polyimide Pyrolysis Conditions on Carbon Molecular Sieve Membrane

Properties, Industrial & Engineering Chemistry Research 35(9) (1996) 2999-3003. https://doi.org/10.1021/ie950746j

[46] M. Campo, Carbon molecular sieve membranes for gas separation: Study, Preparation and Characterization, University of Porto, Porto, 2009.

Received on 07-11-2022 Accepted on 05-12-2022 Published on 09-12-2022

DOI: https://doi.org/10.15379/2410-1869.2022.11